Available online at www.sciencedirect.com
ScienceDirect
Quaternary Research 69 (2008) 421–437
QUATERNARY RESEARCH
www.elsevier.com/locate/yqres

Origin, weathering, and geochemical composition of loess in southwestern Hungary

Gábor Újvári [a,*], Andrea Varga [b], Zsuzsanna Balogh-Brunstad [c]

[a] Geodetic and Geophysical Research Institute, Hungarian Academy of Sciences, Csatkai E. u. 6-8., H-9400 Sopron, Hungary
[b] Department of Petrology and Geochemistry, Eötvös Loránd University, Pázmány Péter sétány 1/c., H-1117 Budapest, Hungary
[c] School of Earth and Environmental Sciences, Washington State University, Pullman, WA 99164-2812, USA

Received 22 February 2007
Available online 25 April 2008

Abstract

Loess geochemistry generally reflects paleo-weathering conditions and it can be used to determine the average composition of the upper continental crust (UCC). In this study, major and trace element concentrations were analyzed on loess samples from southwestern Hungary to determine the factors influencing their chemical compositions and to propose new average loess compositions. All studied loess samples had nearly uniform chemical composition, suggesting similar alteration history of these deposits. Chemical Index of Alteration values (58–69) suggested a weak to moderate degree of weathering in a felsic source area. Typical non-steady state weathering conditions were shown on the Al_2O_3–$CaO+Na_2O$–K_2O patterns, indicating active tectonism of the Alpine–Carpathian system during the Pleistocene. Whole-rock element budgets were controlled by heavy minerals derived from a felsic magmatic or reworked sedimentary provenance. Geochemical parameters indicated that dust particles must have been recycled and well homogenized during fluvial and eolian transport processes.

Keywords: Loess; Geochemistry; Global average loess estimate; Pleistocene; Central Europe

Introduction

Eolian deposits, such as loess, are studied extensively in Earth sciences because they are potential indicators of paleoclimatic change via preserved fossils, magnetic susceptibility or chemical compositions (e.g. Gallet et al., 1996; Jahn et al., 2001). In addition, the loess geochemical data can be used to determine the average composition of the upper continental crust (UCC; Taylor et al., 1983; Taylor and McLennan, 1985; Gallet et al., 1998; McLennan, 2001). Loess deposits are widespread and cover about 10% of the Earth's surface (Pécsi, 1990). Special attention has been paid to western European, Alaskan, South American, Indian and Chinese loess deposits to investigate geologic setting, geochemical composition, paleoclimatic records and the origin and provenance of these deposits (Taylor et al., 1983; Lautridou et al., 1984; Gallet et al., 1998; Tripathi and Rajamani, 1999; McLennan, 2001; Sun, 2002; Roddaz et al., 2006; Schellenberger and Veit, 2006). Factors leading to the deposition of loess–paleosol sequences in Hungary and contributing to their internal geochemical variability, however, have not been investigated in detail. Previous geochemical studies of Hungarian loess deposits analyzed only for major elements were not placed into paleoenvironmental framework (Sümeghy, 1953; Pécsi, 1967; Pécsi-Donáth, 1985). Based on major and trace element geochemistry of loess–paleosol series in Transdanubia, Hum and Fényes (1995) and Hum (1998a, 1998b, 2002) suggested that reconstruction of paleoclimatic trends is possible. However, these authors described geochemical data without any modern provenance and paleo-weathering interpretations.

Previous source area interpretations identified 3 main sources of loess deposits in Hungary (Fig. 1a): (I) glacial materials carried through the Moravian Depression by glacial floodwater, (II) weathering products of the Carpathian Flysch, and (III) glacial materials from the Alpine region (Smalley and Leach, 1978; Pécsi, 1993). An alternative explanation was offered by Smith et al. (1991), who inferred a dominantly local source for Hungarian loess, suggesting that the Pannonian

* Corresponding author. Fax: +36 99 508 355.
E-mail address: ujvari@ggki.hu (G. Újvári).

0033-5894/$ - see front matter © 2008 University of Washington. All rights reserved.
doi:10.1016/j.yqres.2008.02.001

deposits (marine and shallow lacustrine deposits of conglomerates, sandstones, clays, marls, and sands) occuring subsurface in the Great Hungarian Plain (about 40–200 km around the sections, Fig. 1a), formed in the Pannonian s.l. epoch (equivalent to Pliocene and upper part of Miocene, ~1.8–12.6 Ma; Rónai, 1985) could theoretically contribute materials to the loess deposits. On the other hand, Wright (2001) emphasized the cumulative effects of several silt-sized quartz-producing mechanisms (aeolian abrasion, fluvial comminution, glacial grinding, frost weathering) and sorting processes during the formation of loess deposits in Hungary on the basis of previous laboratory simulations (Wright et al., 1998). She suggested that the source rocks of these loess deposits might be originating north of the Moravian Depression and local, possibly Pannonian sediments (Fig. 1a).

Geochemical studies of fine-grained sediments have contributed significantly to the determination of the average upper continental crust composition (Taylor and McLennan, 1985, Schnetger, 1992; Gallet et al., 1996, 1998; McLennan, 2001). Schnetger (1992) presented an average loess composition (AVL^1) including the values for seven loess regions from a variety of depositional scales, and McLennan (2001) redetermined an average Quaternary loess composition (AVL^2) from the mean of eight regional loess averages from New Zealand, central North America, Kaiserstuhl region (Germany), Spitsbergen (Norway), Argentina, United Kingdom, France, and China.

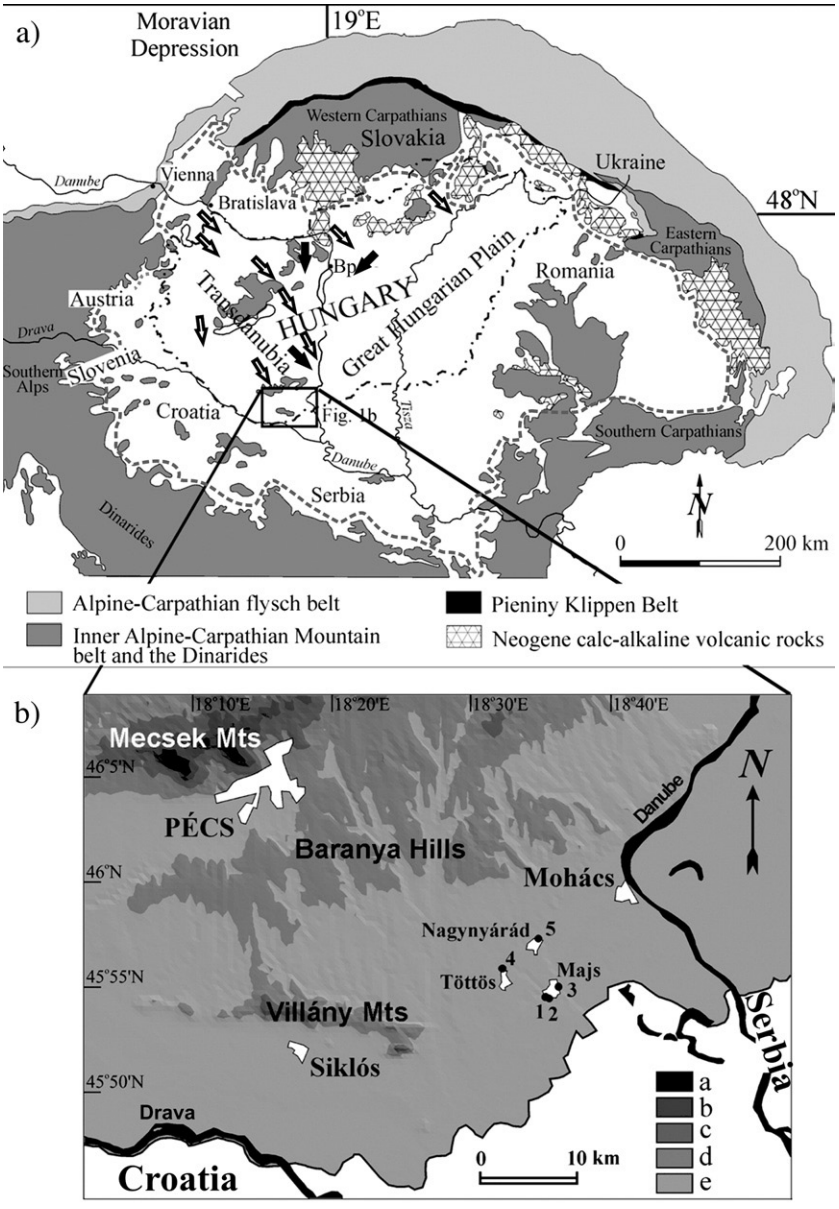

Figure 1. a) Geological framework of the Carpathian–Pannonian area (modified from Csontos et al., 1992, 2002). Gray, dashed line outlines the area of the Pannonian (Carpathian) Basin, black dot-dashed line indicates the border of Hungary; black arrows show paleo-wind directions from Bradák (in press), white arrows indicate paleo-wind directions from Jámbor (2002). Bp. = Budapest; b) Enlarged boxed area; the generalized topographical map of the study area with sampling localities. Sample locations: 1 — Majs 2/a section; 2 — Majs 2/b section; 3 — Majs 3 section; 4 — Töttös section; 5 — Nagynyárád section. Map legend with elevation intervals: a) 475 to 577 m; b) 375 to 475 m; c) 270 to 375 m; d) 170 to 270 m; e) 70 to 170 m.

https://doi.org/10.1016/j.yqres.2008.02.001 Published online by Cambridge University Press

Detailed geochemical investigations of loess deposits worldwide contribute to the accurate determination of average loess composition, which is particularly fruitful in establishing the average composition of the upper continental crust (Taylor et al., 1983; Taylor and McLennan, 1985, Schnetger, 1992; Gallet et al., 1996, 1998; McLennan, 2001).

In this study, major and trace element concentrations were analyzed on loess samples from southwestern Hungary (Fig. 1b) with the following main objectives: (a) to provide a detailed geochemical characterization of the loess deposits in southwestern Hungary and to compare the results with those of previous geochemical investigations for other loess deposits elsewhere in the world; (b) to evaluate the nature, origin, and provenance of the Hungarian loess deposits along with the main factors influencing the chemical composition of these sediments; and (c) to provide a contribution to a worldwide database on the chemical composition of loess deposits and to propose a new average loess composition. Here, we determined the new average loess composition from existing data of 11 loess regions with more than 25 sampling sites (AVL^3; $n=192$). Furthermore, we complemented AVL^3 with our present data of loess composition from southwestern Hungary and the new estimates could be adapted as a global average loess composition (GAL).

Geological setting

Hungary is located in the central Carpathian–Pannonian basin (Fig. 1a). In southwestern Hungary, Baranya County is covered by Neogene–Quaternary unconsolidated sediments, including Pleistocene loess deposits of great thickness (20–60 m). The northern and northwestern portions of the study area are part of the Baranya Hills and its southern and southeastern portions are part of the terraced alluvial fan system of the Danube River (Fig. 1b).

Two lithologic units have been distinguished within the Hungarian loess deposits: (1) Young Loess Series (~16–280 ka; MIS 2–8) and (2) Old Loess Series (~280–900 ka; MIS 9–24) (Pécsi, 1995; Shackleton et al., 1990). The Young Loess Series can be subdivided to Dunaújváros–Tápiósüly (upper part) and Mende–Basaharc (lower part) sequences (Pécsi, 1993). Old Loess Series includes the lower and upper parts of the Paks sequence (Pécsi, 1993, 1995). Based on biostratigraphic data and a single ^{14}C age (33270±1140 ^{14}C yr BP, Majs 2/b depth 2.40 m; Újvári, 2005), the studied sections represent the middle to late Pleistocene interval, corresponding to the lower and upper parts of the Young Loess Series (Fig. 2).

The mineral composition of the Pleistocene Young Loess Series from southeastern Transdanubia is mainly silt-sized quartz (31.1–48.8%), feldspars (5.2–13.6%), carbonate minerals and a minor proportion of micas and heavy minerals (Hum and Fényes, 1995; Hum, 2002). The clay-mineral assemblage consists predominantly of illite and chlorite with minor proportions of smectite, kaolinite, mixed-layer illite/smectite, and rare mixed-layer chlorite/smectite. These loess deposits have high carbonate content (10.7–38.2%) with an average value of 24.4%. Within the carbonate fraction, the dolomite content is unusually high (69.4% in average) and the calcite/dolomite ratio is 1:2 (Hum and Fényes, 1995; Hum, 2002), which is reversed compare to the other loess deposits in the world, where the calcite/dolomite ratio is 2:1 or 3:1 (Hädrich, 1975; Pye, 1983; Taylor et al., 1983, Schnetger, 1992). Hum and Fényes (1995) suggested that that high dolomite content is "primary" and thus they traced it back to the special composition of source rocks.

Methodology

Sampling and analytical methods

The best exposures of the Pleistocene loess deposits of southeastern Transdanubia occur in the southeastern part of the Baranya Hills, where natural outcrops, roadcuts and loam pits expose parts of the Young Loess Series. A total of 54 loess samples were collected from 5 sampling locations (Fig. 1b). The sediment thickness ranged from 2.8 to 6.4 m in the profiles (Fig. 2). Vertical interval of sampling was 40 cm at each site. The samples were numbered from top to bottom, so the numbering increases downwards in the profile. It is beyond the scope of this study to discuss the effects of soil-forming processes, and so two samples (N-4 and N-5, Nagynyárád section) collected from a humus horizon (loess syrosem) were excluded.

The samples were analyzed for major and trace element abundances with X-ray fluorescence spectrometry (XRF) using

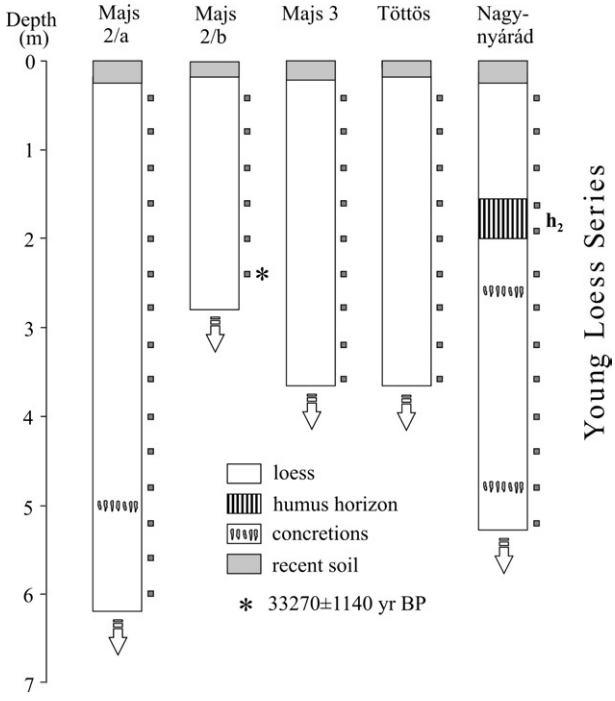

Figure 2. The studied loess profiles and their stratigraphic position. Positions of samples are indicated by the little grey squares to the right of each section. The "0" m indicates the top of the sequences which are uncorrelated in time, i.e. the ages of loesses are not necessarily the same. h_2 is the abbreviation of humus horizon (loess syrosem) in Hungarian loess–paleosol lithostratigraphy (Pécsi, 1995). Asterisk (*) indicates the sample gave a ^{14}C age of 33270±1140 yr BP (code: deb-11500, Laboratory of Environmental Studies, Institute of Nuclear Research of the Hungarian Academy of Sciences, Debrecen). Broken arrows denote that the subsurface rocks are also loess deposits.

https://doi.org/10.1016/j.yqres.2008.02.001 Published online by Cambridge University Press

Table 1
Major (wt%) and trace element (ppm) concentrations of the Hungarian loess samples from southwestern Hungary (Young Loess Series)

Section	Majs 2/a																	
Sample	M2/a-1	M2/a-2	M2/a-3	M2/a-4	M2/a-5	M2/a-6	M2/a-7	M2/a-8	M2/a-9	M2/a-10	M2/a-11	M2/a-12	M2/a-13	M2/a-14	M2/a-15	M2/a-16	Mean	St.D.
Sample No.	020	021	022	023	024	025	026	027	028	029	030	031	032	033	034	035		
Depth (m)	0.40	0.80	1.20	1.60	2.00	2.40	2.80	3.20	3.60	4.00	4.40	4.80	5.20	5.60	6.00	6.40		
Type	L	L	L	L	L	L	L	L	L	L	L	L	L	L	L	L		
SiO_2	62.49	53.63	58.22	59.90	62.10	65.50	64.94	63.97	63.71	61.73	61.95	60.68	63.54	61.99	62.67	61.60	61.8	2.8
TiO_2	0.88	0.76	0.83	0.87	0.94	0.97	0.94	0.92	0.90	0.87	0.87	0.85	0.90	0.87	0.88	0.86	0.9	0.0
Al_2O_3	12.32	10.56	11.33	12.12	13.75	14.78	14.12	13.57	13.31	12.67	12.44	12.60	13.14	12.75	12.68	12.45	12.8	1.0
FeO_{tot}	4.35	3.78	3.96	4.33	4.85	5.13	4.67	4.47	4.33	4.22	4.11	4.41	4.29	4.15	4.26	4.28	4.3	0.3
MnO	0.11	0.08	0.09	0.09	0.10	0.10	0.10	0.09	0.09	0.09	0.09	0.09	0.09	0.09	0.09	0.09	0.1	0.0
MgO	3.20	4.40	5.02	4.95	4.31	2.97	2.57	2.85	3.10	4.02	4.52	4.56	4.41	4.67	4.74	4.92	4.1	0.8
CaO	12.49	23.50	16.96	13.98	9.73	6.09	8.52	10.11	10.56	12.49	12.03	12.84	9.51	11.38	10.47	11.64	12.0	3.9
Na_2O	1.28	1.14	1.35	1.40	1.60	1.65	1.50	1.47	1.46	1.43	1.51	1.45	1.53	1.50	1.63	1.64	1.5	0.1
K_2O	2.27	1.89	2.04	2.18	2.42	2.58	2.43	2.35	2.35	2.30	2.32	2.34	2.41	2.42	2.42	2.33	2.3	0.2
P_2O_5	0.62	0.27	0.21	0.20	0.21	0.21	0.21	0.19	0.19	0.17	0.17	0.17	0.18	0.18	0.17	0.19	0.2	0.1
Total	100	100	100	100	100	100	100	100	100	100	100	100	100	100	100	100	100.0	0.0
LOI (%)	13.9	19.9	16.6	15.4	12.2	8.8	10.3	11.2	11.6	13.2	13.5	13.7	11.5	13.3	12.9	13.7	13.2	2.6
CIA	65	65	63	63	64	64	65	65	64	64	63	63	63	63	61	61	63.5	1.2
Rb	98	79	83	91	102	112	111	105	99	93	90	93	98	95	93	88	96	9
Sr	154	200	204	202	168	156	146	161	168	201	210	221	195	231	241	239	194	31
Ba	402	340	346	365	436	456	437	417	416	387	401	402	411	423	388	397	402	32
Pb	18	15	16	15	19	19	19	17	16	14	18	17	18	19	16	16	17	2
Th	15	11	11	14	14	14	14	14	13	14	13	12	14	15	14	14	14	1
Zr	362	315	351	359	356	365	368	366	368	363	368	348	366	352	371	361	359	13
Nb	18	17	16	17	19	20	18	18	18	17	18	17	18	17	17	16	17	1
La	42	35	46	52	46	54	50	60	55	40	39	43	43	42	46	48	46	7
Ce	87	73	82	85	81	104	103	95	94	91	89	80	82	91	88	92	89	8
Y	40	33	37	38	41	43	38	38	40	38	38	37	38	36	38	37	38	2
V	83	68	81	76	96	102	82	90	84	92	77	88	89	78	85	89	85	8
Cr	82	61	72	72	77	82	88	77	75	74	73	74	75	76	74	67	75	6
Ni	36	19	27	30	38	42	38	37	35	33	33	33	34	33	32	30	33	5
Cu	24	16	18	19	25	24	19	21	20	18	17	16	18	20	15	13	19	3
Zn	72	60	61	66	71	79	73	72	71	65	61	64	70	66	68	66	68	5
Ga	13	13	14	14	18	17	17	17	16	17	16	14	18	15	17	18	16	2
Rb/Sr	0.64	0.40	0.41	0.45	0.61	0.72	0.76	0.65	0.59	0.46	0.43	0.42	0.50	0.41	0.39	0.37	0.5	0.1
Ba/Sr	2.61	1.70	1.70	1.81	2.60	2.92	2.99	2.59	2.48	1.93	1.91	1.82	2.11	1.83	1.61	1.66	2.1	0.5
La/Th	2.80	3.18	4.18	3.71	3.29	3.86	3.57	4.29	4.23	2.86	3.00	3.58	3.07	2.80	3.29	3.43	3.4	0.5

Section	Majs 2/b									Majs 3											
Sample	M2/b-1	M2/b-2	M2/b-3	M2/b-4	M2/b-5	M2/b-6	M2/b-7	Mean	St.D.	M3-1	M3-2	M3-3	M3-4	M3-5	M3-6	M3-7	M3-8	M3-9	Mean	St.D.
Sample No.	036	037	038	039	040	041	042			043	044	045	046	047	048	049	050	051		
Depth (m)	0.40	0.80	1.20	1.60	2.00	2.40	2.80			0.40	0.80	1.20	1.60	2.00	2.40	2.80	3.20	3.60		
Type	L	L	L	L	L	L	L			L	L	L	L	L	L	L	L	L		
SiO_2	61.92	67.36	69.84	65.55	71.10	71.07	63.70	67.2	2.6	57.54	58.20	63.32	64.56	65.74	65.49	65.76	65.37	63.31	63.3	3.2
TiO_2	0.91	0.99	0.98	0.92	0.99	0.98	0.88	1.0	0.0	0.82	0.84	0.94	0.92	0.92	0.93	0.96	0.95	0.91	0.9	0.1

Al_2O_3	13.75	14.95	14.97	13.85	14.74	14.72	12.70	14.2	0.6	11.16	11.49	13.83	13.65	13.74	13.68	14.28	14.32	13.67	13.3	1.2
FeO_{tot}	4.82	5.28	5.03	4.66	4.94	4.88	4.21	4.8	0.2	4.09	4.14	5.00	4.86	4.67	4.64	5.02	4.76	4.75	4.7	0.3
MnO	0.10	0.10	0.10	0.09	0.09	0.09	0.11	0.1	0.0	0.08	0.09	0.10	0.10	0.10	0.10	0.10	0.10	0.09	0.1	0.0
MgO	3.60	2.60	2.32	2.82	2.26	2.31	4.38	2.9	0.5	4.60	4.74	4.24	3.74	3.82	3.69	3.80	3.14	3.79	4.0	0.5
CaO	10.66	4.41	2.44	8.04	1.38	1.26	9.23	5.3	3.0	18.05	16.89	8.15	7.79	6.69	7.29	5.76	7.23	9.59	9.7	4.5
Na_2O	1.48	1.57	1.59	1.47	1.67	1.73	1.86	1.6	0.1	1.31	1.32	1.65	1.67	1.67	1.60	1.65	1.53	1.42	1.5	0.2
K_2O	2.55	2.56	2.55	2.40	2.65	2.76	2.75	2.6	0.1	2.12	2.11	2.56	2.49	2.43	2.37	2.44	2.40	2.27	2.4	0.2
P_2O_5	0.21	0.19	0.18	0.19	0.18	0.20	0.17	0.2	0.0	0.23	0.20	0.20	0.22	0.21	0.21	0.22	0.21	0.20	0.2	0.0
Total	100	100	100	100	100	100	100	100.0	0.0	100	100	100	100	100	100	100	100	100	100.0	0.0
LOI (%)	12.4	7.5	6.1	9.9	5.1	4.6	11.9	8.2	2.4	17.3	16.3	10.7	10.0	9.4	9.8	9.2	10.0	13.1	11.8	3.1
CIA	64	65	65	65	64	64	58	63.9	1.4	63	63	63	62	63	64	64	65	66	63.6	1.1
Rb	104	120	122	112	117	111	90	111	7	84	86	103	100	106	105	111	114	107	102	10
Sr	177	160	142	195	127	127	187	159	20	234	244	173	178	175	181	171	191	204	195	27
Ba	426	459	452	438	446	433	393	435	13	355	357	423	420	425	428	420	444	427	411	32
Pb	18	21	20	16	20	15	13	18	2	17	18	18	19	16	17	20	16	15	17	2
Th	14	14	17	15	15	15	16	15	1	10	11	14	14	15	15	14	14	14	13	2
Zr	352	383	394	373	409	405	370	384	14	345	348	355	364	368	376	372	372	363	363	11
Nb	17	20	19	18	19	19	17	18	1	16	15	17	15	18	16	17	17	17	16	1
La	48	57	42	59	52	40	43	49	5	55	54	42	62	51	39	49	51	30	48	10
Ce	88	102	100	87	93	91	96	94	4	88	90	90	83	82	78	92	105	98	90	8
Y	39	42	41	41	41	42	37	40	1	35	37	41	40	40	38	40	40	39	39	2
V	89	99	108	98	96	94	80	95	5	80	79	92	103	93	88	106	100	96	93	9
Cr	80	88	90	82	88	85	74	84	4	67	71	79	74	77	81	82	88	82	78	6
Ni	37	41	45	39	42	45	37	41	2	26	28	39	34	37	36	40	38	36	35	5
Cu	21	22	24	19	19	24	19	21	2	15	15	21	19	26	20	18	20	23	20	4
Zn	75	76	78	76	78	77	65	75	3	58	61	77	73	85	74	76	77	73	73	8
Ga	17	18	17	16	19	19	15	17	1	15	14	16	17	16	18	16	19	17	16	2
Rb/Sr	0.59	0.75	0.86	0.57	0.92	0.87	0.48	0.7	0.1	0.36	0.35	0.60	0.56	0.61	0.58	0.65	0.60	0.52	0.5	0.1
Ba/Sr	2.41	2.87	3.18	2.25	3.51	3.41	2.10	2.8	0.4	1.52	1.46	2.45	2.36	2.43	2.36	2.46	2.32	2.09	2.2	0.4
La/Th	3.43	4.07	2.47	3.93	3.47	2.67	2.69	3.2	0.5	5.50	4.91	3.00	4.43	3.40	2.60	3.50	3.64	2.14	3.7	1.1

Section	Töttös											Nagynyárád														
Sample	T-1	T-2	T-3	T-4	T-5	T-6	T-7	T-8	T-9	Mean	St.D.	N-1	N-2	N-3	N-4	N-5	N-6	N-7	N-8	N-9	N-10	N-11	N-12	N-13	Mean	St.D.
Sample No.	052	053	054	055	056	057	058	059	060			061	062	063	064	065	066	067	068	069	070	071	072	073		
Depth (m)	0.40	0.80	1.20	1.60	2.00	2.40	2.80	3.20	3.60			0.40	0.80	1.20	1.60	2.00	2.40	2.80	3.20	3.60	4.00	4.40	4.80	5.20		
Type	L	L	L	L	L	L	L	L	L			L	L	L	HL	HL	L	L	L	L	L	L	L	L		
SiO_2	53.37	55.47	57.85	62.64	64.72	68.46	69.22	69.72	65.54	63.0	6.1	68.01	69.23	62.40	61.94	64.89	57.36	58.39	59.68	60.63	61.02	58.99	65.40	59.71	62.1	3.7
TiO_2	0.75	0.79	0.83	0.94	0.96	1.01	1.01	0.99	0.93	0.9	0.1	1.00	1.01	0.92	0.92	0.95	0.80	0.83	0.90	0.88	0.86	0.82	0.93	0.85	0.9	0.1
Al_2O_3	10.74	11.10	11.84	13.91	14.95	15.90	15.59	15.29	14.07	13.7	2.0	15.29	15.20	14.08	13.92	14.64	11.53	12.19	13.67	12.84	12.62	12.60	10.30	12.46	13.2	1.5
FeO_{tot}	3.88	4.06	4.17	4.99	5.32	5.58	5.46	5.31	4.86	4.8	0.7	5.48	5.28	5.02	4.99	5.17	4.15	4.43	5.03	4.60	4.51	4.29	3.34	4.49	4.7	0.6
MnO	0.07	0.08	0.08	0.11	0.11	0.11	0.11	0.10	0.10	0.1	0.0	0.11	0.10	0.09	0.10	0.10	0.08	0.08	0.10	0.09	0.09	0.09	0.08	0.09	0.1	0.0
MgO	4.20	4.55	4.65	3.90	3.38	2.29	2.25	2.47	3.59	3.5	0.9	2.26	2.36	3.68	4.18	3.12	2.92	3.91	4.07	3.97	4.16	4.41	4.38	4.80	3.7	0.8
CaO	23.59	20.57	16.98	9.47	6.24	2.33	2.03	1.87	6.92	10.0	8.3	3.63	2.71	9.90	9.93	7.01	20.12	16.81	12.82	13.34	13.04	15.19	12.01	13.95	11.6	5.0
Na_2O	1.08	1.16	1.31	1.44	1.56	1.54	1.56	1.51	1.41	1.4	0.2	1.59	1.54	1.44	1.52	1.51	0.94	1.11	1.22	1.23	1.24	1.21	1.52	1.23	1.3	0.2
K_2O	1.95	1.96	2.07	2.39	2.53	2.58	2.56	2.53	2.41	2.3	0.3	2.45	2.38	2.31	2.33	2.45	1.95	2.09	2.34	2.26	2.30	2.25	1.84	2.25	2.2	0.2
P_2O_5	0.37	0.27	0.22	0.22	0.23	0.22	0.22	0.20	0.19	0.2	0.1	0.17	0.19	0.17	0.17	0.16	0.15	0.16	0.16	0.16	0.15	0.15	0.19	0.17	0.2	0.0
Total	100	100	100	100	100	100	100	100	100	100.0	0.0	100	100	100	100	100	100	100	100	100	100	100	100	100	100.0	0.0
LOI (%)	19.5	18.1	16.7	11.8	9.5	6.1	5.9	5.8	9.9	11.5	5.4	7.0	6.2	12.0	11.9	9.8	17.6	16.0	13.9	14.0	14.0	15.7	12.7	14.9	12.7	3.4

(continued on next page)

Table 1 (*continued*)

Section	Töttös											Nagynyárád														
Sample	T-1	T-2	T-3	T-4	T-5	T-6	T-7	T-8	T-9	Mean	St.D.	N-1	N-2	N-3	N-4	N-5	N-6	N-7	N-8	N-9	N-10	N-11	N-12	N-13	Mean	St.D.
Sample No.	052	053	054	055	056	057	058	059	060			061	062	063	064	065	066	067	068	069	070	071	072	073		
Depth (m)	0.40	0.80	1.20	1.60	2.00	2.40	2.80	3.20	3.60			0.40	0.80	1.20	1.60	2.00	2.40	2.80	3.20	3.60	4.00	4.40	4.80	5.20		
Type	L	L	L	L	L	L	L	L	L			L	L	L	HL	HL	L	L	L	L	L	L	L	L		
CIA	66	65	64	66	66	67	66	67	66	65.8	0.8	66	67	66	65	66	69	67	68	66	66	66	60	66	65.9	2.2
Rb	82	81	88	104	116	125	124	122	108	106	18	117	116	106	103	112	91	93	107	98	99	97	73	99	101	12
Sr	198	210	225	174	159	139	131	127	155	169	36	144	136	180	192	168	198	201	212	207	231	249	223	216	197	33
Ba	332	361	371	431	459	473	485	469	429	423	56	462	450	427	420	457	365	369	442	404	429	396	326	388	410	41
Pb	15	16	14	21	19	20	21	21	19	18	3	21	20	19	17	17	14	20	22	18	18	17	15	17	18	2
Th	14	12	14	16	15	17	15	17	11	15	2	15	14	15	15	15	13	14	13	15	15	12	14	15	14	1
Zr	308	323	342	356	359	379	391	396	375	359	30	388	409	351	353	369	341	345	343	357	352	326	502	347	368	46
Nb	16	17	17	18	19	21	20	20	18	18	2	19	20	18	18	19	17	17	17	17	16	16	16	15	17	1
La	53	41	34	35	60	56	54	55	44	48	10	52	56	60	66	37	52	48	63	31	52	40	50	62	51	11
Ce	74	82	83	95	92	94	113	99	95	92	11	99	111	82	93	105	88	89	100	96	76	93	102	103	95	10
Y	33	35	36	40	43	43	43	44	40	40	4	43	44	40	40	42	36	36	40	38	36	36	41	36	39	3
V	86	84	92	94	107	112	107	103	102	99	10	101	112	98	108	95	69	86	98	79	96	85	76	90	92	13
Cr	69	71	76	85	90	99	99	96	84	85	12	92	97	86	81	87	74	77	84	76	79	77	66	80	81	8
Ni	25	27	29	39	46	49	47	47	43	39	10	47	49	43	39	43	30	32	37	34	33	34	24	33	37	7
Cu	16	13	20	22	23	25	24	25	23	21	4	22	22	21	21	28	16	20	21	20	16	16	8	18	19	5
Zn	57	58	61	74	76	81	81	82	74	72	10	81	79	72	73	78	58	61	75	68	65	67	46	66	68	10
Ga	15	16	15	18	19	19	20	18	17	17	2	18	18	17	16	18	15	18	18	15	17	15	13	19	17	2
Rb/Sr	0.41	0.39	0.39	0.60	0.73	0.90	0.95	0.96	0.70	0.7	0.2	0.81	0.85	0.59	0.54	0.67	0.46	0.46	0.50	0.47	0.43	0.39	0.33	0.46	0.5	0.2
Ba/Sr	1.68	1.72	1.65	2.48	2.89	3.40	3.70	3.69	2.77	2.7	0.8	3.21	3.31	2.37	2.19	2.72	1.84	1.84	2.08	1.95	1.86	1.59	1.46	1.80	2.2	0.6
La/Th	3.79	3.42	2.43	2.19	4.00	3.29	3.60	3.24	4.00	3.3	0.6	3.47	4.00	4.00	4.40	2.47	4.00	3.43	4.85	2.07	3.47	3.33	3.57	4.13	3.6	0.7

L: loess; HL: humic loess or loess syrosem; St.D.: standard deviation; LOI: Loss on ignition; CIA: Chemical Index of Alteration (Nesbitt and Young, 1982).
Total iron expressed as FeO. Major element data are recalculated on a volatile-free basis.

a Rigaku 3370 XRF Spectrometer, following the procedure of Johnson et al. (1999) in the GeoAnalytical Laboratory of the Washington State University, Pullman, WA, USA.

In short, rock samples were prepared for analyses in a swing mill in tungsten carbide bowls to a very fine powder, weighing with dilithium tetraborate ($Li_2B_40_7$) flux (2:1 flux:rock), mixing with a touch mixer, fusing at 1000°C in a muffle oven, and cooling; each bead was reground, refused and polished on diamond laps to reach a smooth surface. The concentrations of major and trace elements in the unknown samples were measured by comparing the X-ray intensity for each element with the intensity for two beads each of nine USGS standard samples (PCC–1, BCR–1, BIR–1, DNC–1, W–2, AGV–1, GSP–1, G–2 and STM–1) and two beads of pure vein quartz used as blanks for all elements except Si (Johnson et al., 1999). The element concentrations are expressed as wt%, volatile-free, with all the iron expressed as FeO_{tot}. Loss on Ignition (LOI) was obtained by weighing after 16 h of calcination at 900°C. The intensities for all elements were corrected automatically for line interference and absorption effects. Analytical uncertainties are ±2% for the major elements (except Na_2O). Among the trace elements, the precision and therefore the accuracy of Ni, Cr, V, Sc, and Ba was lower than for Rb, Sr, Zr, Nb, Y, Ga, Cu, and Zn. The Ni, Cr, V, Sc, and Ba concentrations are considered only semiquantitative below 30 ppm. The Sc data were not used for analysis, because values were below 30 ppm. The values of Ni were lower than 30 ppm in only 11% of the samples and the values of Cr, V and Ba were higher than 30 ppm, hence these values provided reliable data. Rb, Sr, Zr, Nb, Y, Pb, and Th had satisfactory precision and accuracy down to 1 to 3 ppm. La and Ce data were less precise (2σ: 5.7 and 7.9 ppm, respectively); in spite of this fact the averages of La and Ce values of the 5 sections (54 samples) were found in small range from 46.3 to 51.5 and 88.6 to 95.2, respectively (Table 1).

Geochemical parameters

Geochemical parameters, such as elemental ratios, were determined from the chemical compositions of the sediments. These parameters were used to characterize the geochemical features and evaluate the main factors that influenced their chemical composition. The AVL^3 composition was compared to our loess sample compositions to evaluate differences and similarities between them (Table 2). The potential origins of the loess deposits were determined by including the chemical composition of the possible parent materials, such as flysch sediments and granite from the Western Carpathians (Adamova, 1991; Broska et al., 2002), and molasse sandstones from the Central Alps (von Eynatten, 2003), representing a natural mixture of rocks derived from Alpine provenance area (Austroalpine sedimentary cover, Austroalpine crystalline rocks and Penninic ophiolites) in the comparison process. Other geochemical data from the suggested source areas were unfortunately not available. The supposed connection between the Hungarian loesses and the Pannonian deposits (Smith et al., 1991) could not be investigated because the geochemical analyses of these sediments have not been completed. Upper continental crust (UCC) and post-Archean Australian average shale (PAAS) provided reference compositions (Taylor and McLennan, 1985; McLennan, 2001). The UCC values for TiO_2, V, Cr, Ni, Nb, and Pb were revised by McLennan (2001) compared to the older estimate of Taylor and McLennan (1985).

The degree of subaerial weathering was quantified using the Chemical Index of Alteration (CIA) (Nesbitt and Young, 1982). This index measures the degree of weathering and transformation of feldspars to secondary clay minerals (e.g., kaolinite, illite, and smectite), relative to fresh parent rocks. The index was calculated by the following formula: $CIA = [Al_2O_3/(Al_2O_3 + CaO^* + Na_2O + K_2O)] \times 100$ (in molar proportions). CaO* represents Ca in silicate-bearing minerals only. In this study, we were not able to distinguish carbonate CaO from silicate CaO with our analytical methods, so we adapted the method of McLennan (1993) assuming reasonable Ca/Na ratios in silicate minerals. The CaO∗ concentration was calculated based on the following: (a) if the concentration of CaO was less than or equal to the concentration of Na_2O in the sample, we adopted this CaO value; (b) if the CaO concentrations were higher than the Na_2O concentrations in the sample, we assumed that the CaO* value was equal to the Na_2O value (Bock et al., 1998; Gallet et al., 1998; Roddaz et al., 2006).

Lastly, we estimated the global average loess composition (GAL) by giving equal weight to each of the regional averages following the method of McLennan (2001) (Table 2).

Results

Major element abundances

Major element concentrations are presented in Table 1. Loss on ignition (LOI) varied from 4.6 wt% to 19.9 wt% and showed a positive correlation with total CaO ($r = 0.99$) in all samples. This suggested that LOI was associated with carbonate minerals, but clay minerals and organic matter may have also played a minor role in the LOI budget. Compositional variations among samples were low to moderate (Table 1). On average, the samples contained a relatively low and narrow range of SiO_2 from 61.8±2.8 wt% (Majs 2/a) to 67.2±2.6 wt% (Majs 2/b). The Al_2O_3 content of the samples showed a narrow range from 12.8±1.0 wt% (Majs 2/a) to 14.2±0.6 wt% (Majs 2/b). On the other hand, a relatively high TiO_2 content (0.9–1.0 wt%) characterizes the loess deposits. CaO content varied widely between 5.3±3.0 and 12.0±3.9 wt%. The samples had low Na_2O from 1.3±0.2 wt% (Nagynyárád) to 1.6±0.1 wt% (Majs 2/b) and relatively low K_2O concentrations from 2.2±0.2 wt% to 2.6±0.1 wt% (Table 1).

Increased SiO_2 content was accompanied by increased Al_2O_3 content (Table 1; Fig. 3a), indicating the presence of abundant aluminosilicate minerals in the loess assemblage, such as feldspars and micas. Our loess SiO_2 and Al_2O_3 concentrations plot close to the composition of slightly weathered crustal rocks (i.e., UCC (Taylor and McLennan, 1985) and granite (Broska et al., 2002)) but far from the relatively altered sedimentary deposits, namely PAAS (Taylor and McLennan, 1985), flysch sediments (Adamova, 1991), and molasse

https://doi.org/10.1016/j.yqres.2008.02.001 Published online by Cambridge University Press

Table 2
Regional averages of major and trace elements in loess and average loess compositions

No.	1	2	3	4	5	6	7	8	9	10	11	12	13	14	15	16	17	-	1-8	1-16	1-17
Locality	[a]NZ	[b]GER[1]	[c]USA	[d]SB	[e]ARG[1]	[f]UK	[g]FR[1]	[h]CH[1]	[i]GER[2]	[j]FR[2]	[k]CH[2]	[l]ARG[2]	[m]IND	[n]PER	[o]HUN[1]	[p]HUN[2]	[q]HUN[3]	[r]AVL[1]	[s]AVL[2]	**[t]AVL[3]**	**[u]GAL**
No.S.	5	2	4	6	7	1	7	20	15	13	7	75	17	3	6	4	52	-	52	**192**	**244**
SiO_2	73.16	59.90	80.05	77.42	67.19	83.94	77.32	65.69	76.60	81.82	62.89	63.74	71.56	–	63.87	62.75	63.48	76.50	73.08	**71.19**	**70.71**
TiO_2	0.58	0.31	0.67	0.69	0.81	0.57	0.72	0.70	0.68	0.71	0.58	0.95	0.72	–	0.90	0.81	0.91	0.63	0.62*	**0.69**	**0.71**
Al_2O_3	15.02	7.88	10.79	11.87	15.24	8.50	8.43	13.13	8.51	9.18	12.59	17.38	12.50	–	12.41	11.05	13.45	12.50	11.36	**11.63**	**11.74**
FeO_{tot}	3.11	2.78	2.42	3.95	4.37	2.52	2.83	4.38	2.64	3.21	4.33	5.88	4.42	–	4.86	3.57	4.67	2.78	3.29	**3.68**	**3.75**
MnO	0.05	0.07	0.03	0.04	0.13	0.05	0.05	0.10	0.06	0.07	0.09	0.12	0.07	–	0.07	0.08	0.09	0.06	0.06	**0.07**	**0.07**
MgO	0.99	3.91	0.92	0.84	1.53	0.59	1.08	2.36	1.35	0.69	3.84	2.21	1.90	–	3.40	5.15	3.62	1.00	1.53	**2.05**	**2.15**
CaO	1.43	23.00	1.07	0.47	5.42	0.46	6.22	8.86	6.72	1.31	10.91	2.41	4.57	–	11.07	13.00	9.73	1.30	5.87	**6.46**	**6.67**
Na_2O	3.29	0.85	1.58	1.73	2.36	0.96	1.12	1.66	1.18	1.02	1.67	3.38	1.70	–	1.36	1.47	1.47	2.10	1.69	**1.69**	**1.68**
K_2O	2.37	1.30	2.47	2.43	2.31	2.05	1.81	2.51	2.15	1.99	2.32	3.06	2.44	–	2.01	1.93	2.37	2.30	2.16	**2.21**	**2.22**
P_2O_5	–	–	–	0.14	0.16	0.07	0.11	0.16	0.12	–	–	0.21	0.15	–	0.07	0.19	0.20	–	0.13	**0.14**	**0.14**
Rb	83	47	74	77	79	73	61	89	74	–	101	156	–	16	–	–	103	81	73*	**78**	**79**
Sr	304	331	187	147	313	71	156	215	155	129	246	324	144	28	–	400	183	246	215	**210**	**208**
Ba	572	195	681	583	630	332	324	457	349	410	409	588	375	80	–	–	416	582	458*	**427**	**427**
Pb	13.0	4.2	14.2	15.5	16.4	15.0	12.6	18.0	10.1	–	20.0	25.0	–	–	–	8.0	18	13	14.1*	**14**	**15**
Th	10.2	5.6	9.5	6.8	7.6	7.0	6.4	10.9	10.1	–	12.7	–	–	8.6	–	–	14	10	8.6*	**9**	**9**
Zr	366	255	428	278	234	327	357	181	513	–	221	287	296	402	–	–	366	387	302*	**319**	**322**
Nb	16.5	9.1	19.5	14.7	11.0	11.0	12.3	11.7	–	–	13.1	17.0	–	11.1	–	–	18	18	12.7*	**13**	**14**
La	35.4	25.0	34.3	29.3	23.9	19.7	24.9	30.3	31.0	–	35.7	–	–	15.6	–	–	49	35	27.9*	**28**	**29**
Ce	76.3	51.5	77.8	62.0	49.3	43.0	50.8	62.6	72.0	–	71.4	–	–	27.2	–	–	92	78	59	**59**	**61**
Y	24.0	19.0	21.3	21.8	23.6	16.0	23.9	25.5	26.0	–	27.4	40.0	32.2	17.1	–	–	39	25	22	**24**	**26**
Sc	8.1	5.9	5.3	–	–	–	–	11.9	7.0	–	11.7	–	–	–	–	–	–	8	7.8*	**8**	**-**
V	65	40	56	119	105	58	69	99	50	83	–	109	–	86	–	–	93	66	77*	**78**	**79**
Cr	31	42	32	109	36	67	61	69	66	111	–	55	122	49	–	69	81	43	56*	**66**	**67**
Ni	13	24	12	24	16	20	17	34	21	38	–	28	66	–	–	–	37	18	20*	**26**	**27**
Cu	12	14	11	15	18	2	8	30	9	21	–	63	–	–	–	26	20	14	14	**19**	**19**
Zn	56	37	45	64	60	41	38	78	33	–	–	109	–	–	–	53	71	54	52	**56**	**57**
Ga	14	7	10	12	15	8	9	17	–	–	16	–	–	–	–	–	17	13	11	**12**	**12**

Major oxides are in wt%, trace elements in ppm. Total iron expressed as FeO. Major element data are recalculated on a volatile-free basis. No.S., number of samples.
[a]Average of 5 loess samples from Banks Peninsula, New Zealand (Taylor et al., 1983).
[b]Average of 2 loess samples from Kaiserstuhl, Germany (Taylor et al., 1983).
[c]Average of 4 loess samples from Kansas and Iowa, USA (Taylor et al., 1983).
[d]Average of 6 loess samples from Spitsbergen (Gallet et al., 1998).
[e]Average of 7 samples from the borehole at Mercedes, 87 km west from Buenos Aires, Argentina (Gallet et al., 1998).
[f]Loess sample from United Kingdom (Gallet et al., 1998).
[g]Average of 7 samples from Brittany, France (Gallet et al., 1998).
[h]Average of 20 loess samples from Nanking, Luochuan, Xining, Xifeng and Jixian sections, China (Taylor et al., 1983; Gallet et al., 1996; Jahn et al., 2001).
[i]Average of 15 loess samples from Lower Saxony and Hessia, Germany (Schnetger, 1992).
[j]Average of 13 loess samples from Normandy, North-West France (Lautridou et al., 1984).
[k]Average of 7 loess samples from the Loess Plateau along a north–south transect, China (Ding et al., 2001).
[l]Average of 75 loess samples from Las Carreras, NW-Argentina (Schellenberger and Veit, 2006).
[m]Average of 17 loess samples from Rajasthan, India (Tripathi and Rajamani, 1999).
[n]Average of 3 loess samples from Iquitos forebulge, Peru (Roddaz et al., 2006).
[o]Average of 6 loess samples from Hungary (Sümeghy, 1953).
[p]Average of 4 loess samples from southeastern Transdanubia, Hungary (Hum and Fényes, 1995).
[q]Average of 52 loess samples from South-Baranya, Hungary (this study, see Table 1).
[r]Average loess[1] composition from the data of seven loess regions (Schnetger, 1992).
[s]Average loess[2] composition from the mean of eight (1–8) regional averages. The data which are marked with *, originated from McLennan (2001).
[t]Average loess[3] composition from the mean of sixteen (1–16) averages of eleven loess regions (n=192) (on the basis of this study).
[u]Global average loess composition from the mean of seventeen (1–17) averages of eleven loess regions (n=244), including the present samples (Table 1) to supplement the AVL[3] data set (on the basis of this study).

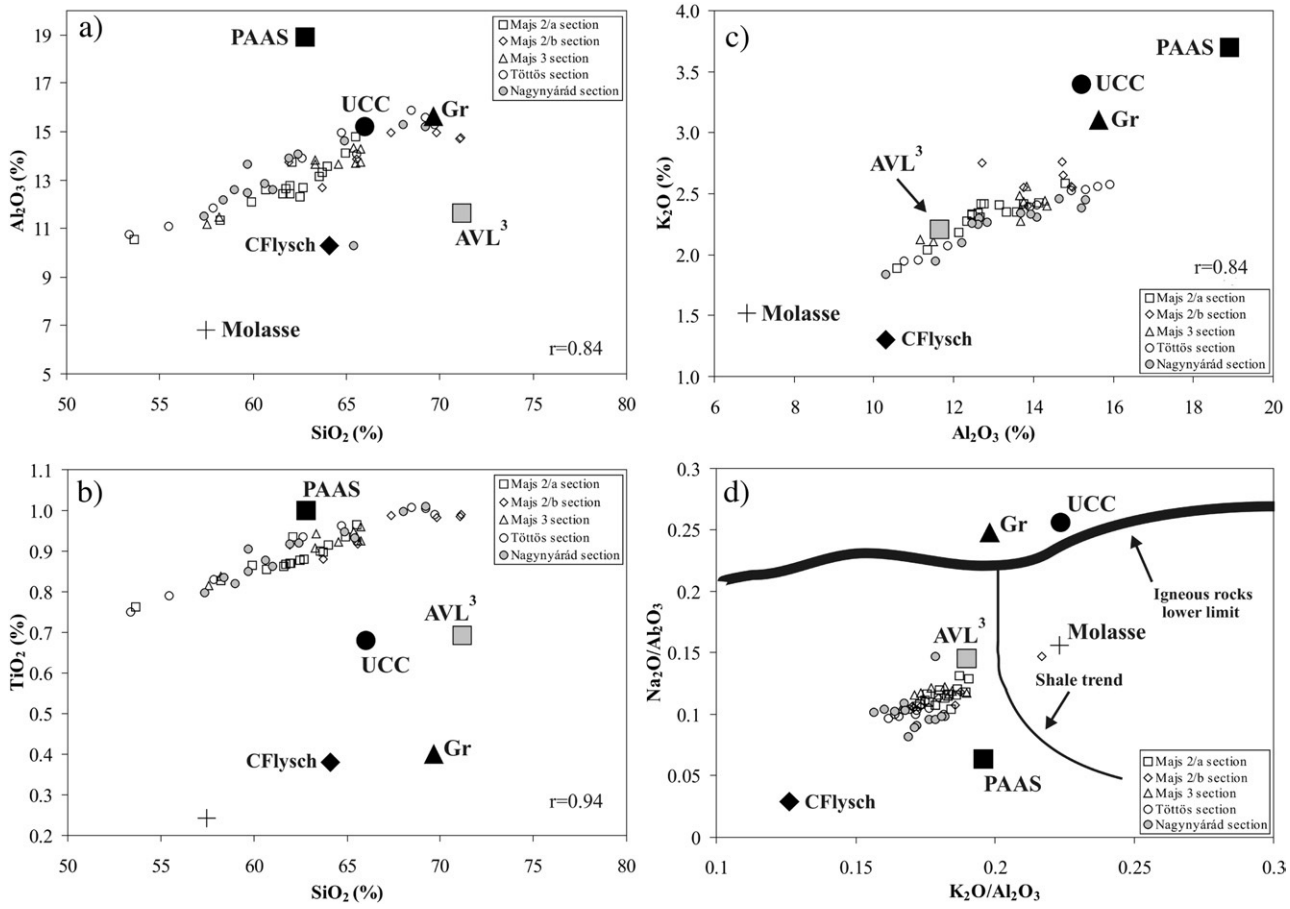

Figure 3. Diagrams of a) Al_2O_3 vs. SiO_2, b) TiO_2 vs. SiO_2, c) K_2O vs. Al_2O_3, and d) Na_2O/Al_2O_3 vs. K_2O/Al_2O_3 comparing the southwestern Hungarian loess samples and average loess composition (AVL^3) (Table 2). Two standards, the post-Archean Australian average shale (PAAS; Taylor and McLennan, 1985; McLennan, 2001) and the Upper Continental Crust (UCC; Taylor and McLennan, 1985; McLennan, 2001), and some potential parent materials, Western Carpathians' granite (Gr; Broska et al., 2002), Carpathian flysch sediments (CFlysch; Adamova, 1991), and sandstones from the Central Alps (Molasse; von Eynatten, 2003) are also shown. Loess samples plot in the sedimentary field under the igneous rocks lower limit (Garrels and Mackenzie, 1971) and left from the shale trend (Gallet et al., 1998) on the Na_2O/Al_2O_3 vs. K_2O/Al_2O_3 diagram.

sandstones (von Eynatten, 2003) (Fig. 3a). The absolute concentrations of the major elements were probably affected by carbonate dilution effect as indicated by the relatively lower ($r=0.84$) correlation between SiO_2 and Al_2O_3 (Fig. 3a).

In addition, the lower SiO_2 content of these Hungarian loess samples relative to the AVL^3 might reflect that these samples had a smaller proportion of silt-sized quartz than other worldwide loess deposits. The strong positive correlation ($r=0.94$) between SiO_2 and TiO_2 (Fig. 3b) suggested that Ti might be bound in small crystals of titanium minerals (e.g., rutile, titanite, and ilmenite) found in the coarse-grained fraction. Nevertheless, the enrichment of TiO_2 was also ascribed to the presence of Ti-bearing phyllosilicates (e.g., biotite and chlorite) corresponding to the average shale (PAAS) composition (Fig. 3b) and the TiO_2 contents in our samples were significantly higher than in UCC and AVL^3. In K_2O vs. Al_2O_3 diagram (Fig. 3c) the samples plotted close to the AVL^3 composition. The clear relationship between these elements ($r=0.84$) suggested that Al_2O_3 abundance was mainly governed by the presence of phyllosilicates and/or K-feldspar. In the diagram of Na_2O/Al_2O_3 vs. K_2O/Al_2O_3 (Fig. 3d) all samples clustered close to the AVL^3 composition, which is diagnostic of depositional conditions of sedimentary rocks that have distinctly lower Na_2O/Al_2O_3 values than igneous rocks (Garrels and MacKenzie, 1971; Gallet et al., 1998). This result confirmed that all particles making up the loess deposits must have undergone previous sedimentary differentiation processes (Gallet et al., 1998).

All sampling sites exhibited similar patterns in the major element compositions normalized to UCC (Fig. 4). The SiO_2, Al_2O_3, and FeO_{tot} contents were similar or slightly lower than in the UCC. The samples were slightly enriched in MnO and significantly enriched in TiO_2 and P_2O_5, except Nagynyárád, where P_2O_5 was about the same as UCC. The high MgO content and low Na_2O and K_2O concentrations were characteristics of our samples. The only distinct difference was found in the CaO content, which was mostly enriched compared to UCC with the largest values among the major elements. A few samples of Majs 2/b, Töttös and Nagynyárád sections were depleted in CaO and pointed toward PAAS composition (Fig. 4b, d, e, f).

The negative anomalies of Na_2O and K_2O were possibly linked to their high mobility during continental weathering (see

https://doi.org/10.1016/j.yqres.2008.02.001 Published online by Cambridge University Press

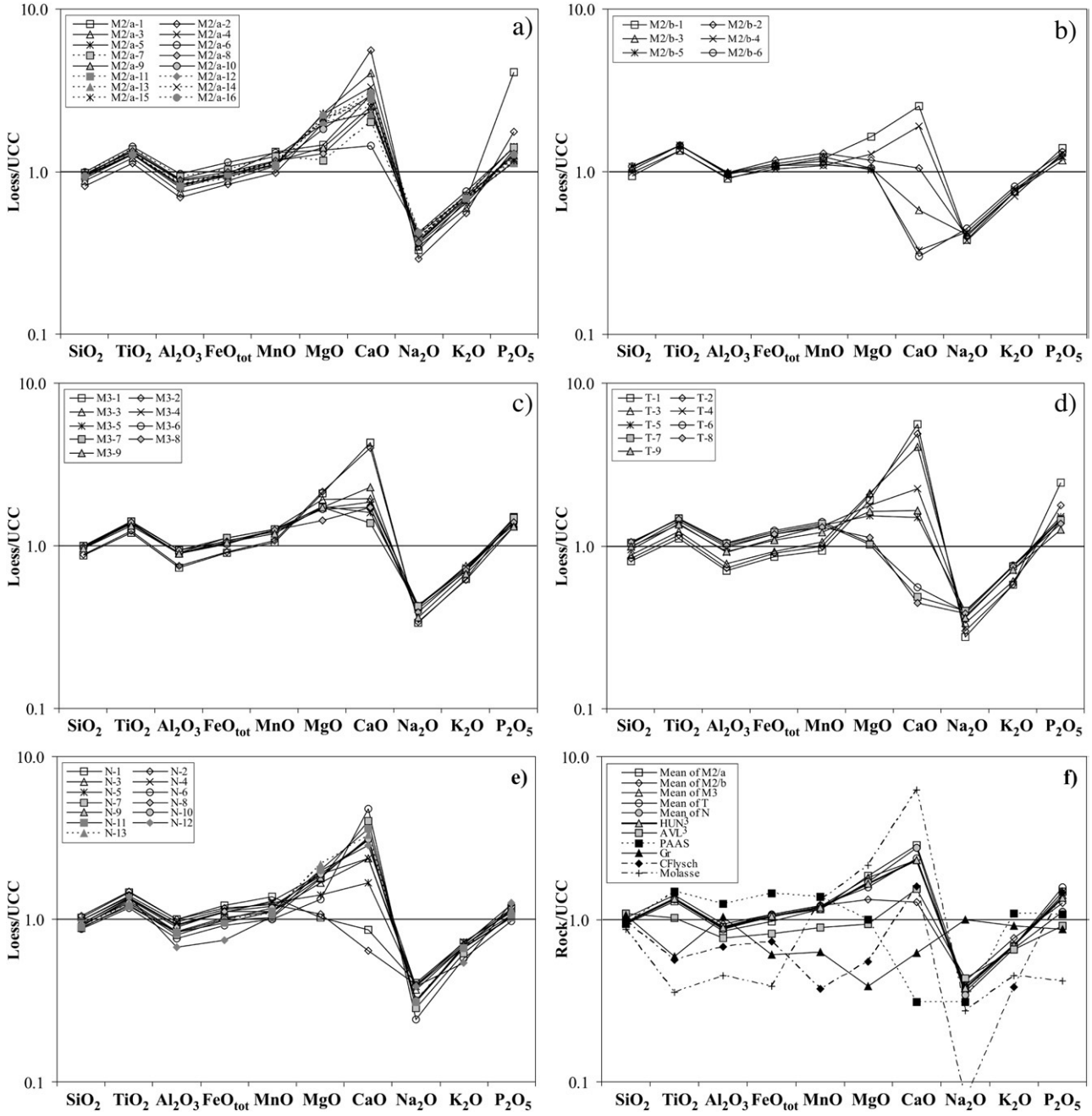

Figure 4. UCC-normalized major element patterns for the loess samples of the five sections a) Majs 2/a, b) Majs 2/b, c) Majs 3, d) Töttös, and e) Nagynyárád (southwestern Hungary); f) shows the mean values of each sections, the Hungarian average (HUN[3]; Table 2), the average loess (AVL[3]; Table 2), and the PAAS standard and potential source materials: Western Carpathians' granite (Gr; Broska et al., 2002), Carpathian flysch sediments (CFlysch; Adamova, 1991), sandstones from the Central Alps (Molasse; von Eynatten, 2003). The UCC and PAAS values were used from Taylor and McLennan (1985) and McLennan (2001).

details below). It is well known that the CaO content of loess varies greatly and shows both positive and negative anomalies on UCC-normalized diagrams (Gallet et al., 1998; Jahn et al., 2001). High carbonate content characterizes many European loess deposits (Taylor et al., 1983), and the lower CaO values may indicate an intensive Ca mobilization during post-depositional processes (Gallet et al., 1996; Jahn et al., 2001). In the present samples, relatively high MgO content reflects the presence of abundant dolomite, confirming previous petrographic results (Pécsi-Donáth, 1985; Hum and Fényes, 1995; Hum, 2002).

Based on the mean values of each site, the UCC-normalized major element distributions of the different profiles were similar to AVL[3] distribution pattern (Fig. 4f). However, our samples were significantly higher in TiO_2, FeO_{tot}, MnO, MgO and CaO, and slightly higher in P_2O_5 than the AVL[3]. On the other hand, the SiO_2, TiO_2, Na_2O and P_2O_5 composition of the present samples were similar to PAAS, but the samples were depleted in

https://doi.org/10.1016/j.yqres.2008.02.001 Published online by Cambridge University Press

Al_2O_3, FeO_{tot}, MnO and K_2O and significantly enriched in MgO and CaO relative to the PAAS (Fig. 4f).

Trace elements

Trace element distribution was more variable among the samples than the major element data (Table 1; Fig. 5). All sections were slightly depleted in Rb and Ba with respect to the large ion lithophile elements (LILEs) and strongly depleted in Sr relative to the UCC (Fig. 5). The Sr depletion was a consequence of its high solubility during weathering (Jahn et al., 2001). In the Ba/Sr vs. Rb/Sr diagram (Fig. 6), the data points of the present samples defined a linear trend from a starting point close to the UCC composition towards the PAAS composition. The high correlation between Ba/Sr vs. Rb/Sr ratios ($r=0.99$) suggested that Rb and Ba abundances were exclusively governed by the various amounts of K-bearing minerals (e.g., K-feldspar, muscovite, and illite).

On average, distribution of the high field strength elements (HFSEs) and the light rare earth elements (LREEs) such as La and Ce displayed a coherent behaviour. The loess samples were enriched in Th, Zr, Nb, La, Ce, and Y relative to the UCC

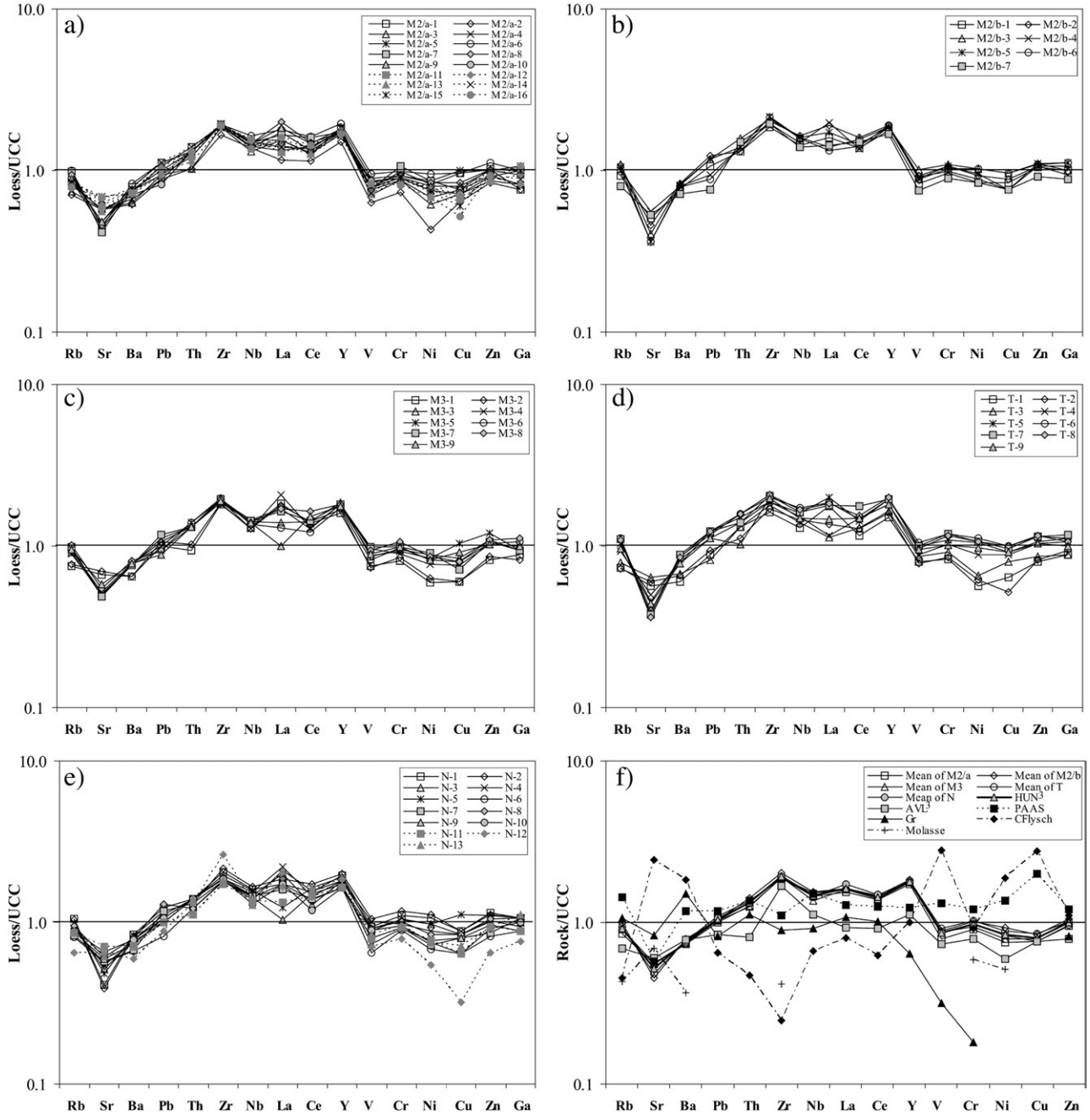

Figure 5. UCC-normalized trace element patterns for the studied loess samples. Abbreviations and symbols as in Figure 4.

https://doi.org/10.1016/j.yqres.2008.02.001 Published online by Cambridge University Press

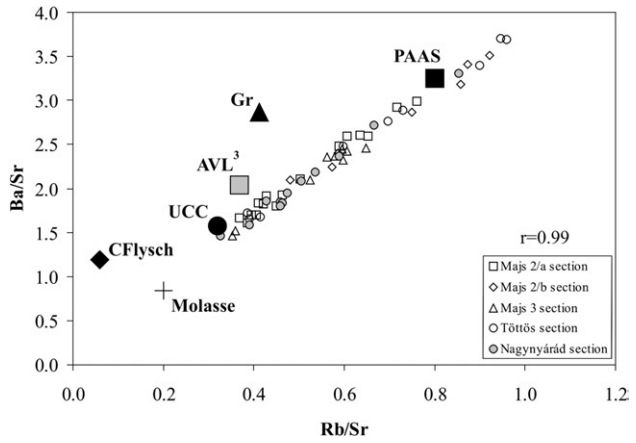

Figure 6. Plot of Ba/Sr vs. Rb/Sr for the studied loess samples (southwestern Hungary). Loess values were compared to average loess composition (AVL[3]; Table 2), post-Archean Australian average shale (PAAS; Taylor and McLennan, 1985; McLennan, 2001), Upper Continental Crust (UCC; Taylor and McLennan, 1985) and three potential source materials: Western Carpathians' granite (Gr; Broska et al., 2002), Carpathian flysch sediments (CFlysch; Adamova, 1991), and sandstones from the Central Alps (Molasse; von Eynatten, 2003).

(Fig. 5). This pattern is similar to the TiO_2 and P_2O_5 data distribution (Fig. 4), suggesting that behaviour of the HFSE and LREE was mainly controlled by the detrital heavy mineral fraction. The samples were slightly depleted in transition trace elements (TTEs) including V, Cr, Ni, Cu, and Zn relative to the UCC. Additionally, they have similar Ga content to the UCC (Fig. 5).

Based on the mean values of each site, the UCC-normalized trace element distributions showed some similarity to the AVL[3] (Fig. 5f). The samples were distinctively higher in Rb, Pb, HFSE (except for Zr), LREE, and TTE (except for V and Cu) averages compared to the AVL[3] composition. On the other hand, they had similar averages of Sr, Pb, Th, Nb and Zn to the PAAS, but they were depleted in LILEs and TTEs (especially in Cu) and enriched in HFSEs (except for Nb) and LREE relative to the PAAS (Fig. 5f).

Discussion

Source area weathering

The degree of chemical weathering is a function of time, climate and erosion rate, the latter of which varies with the rate of tectonic uplift (Nesbitt et al., 1997). A common approach to quantify the degree of subaerial weathering is to use the Chemical Index of Alteration (CIA) (Nesbitt and Young, 1982). However, the CIA by itself cannot distinguish between "old" and "recent" weathering events. The CIA values for unweathered plagioclase and K-feldspars are approximately equal to 50, similarly to values of fresh upper crustal rocks. The CIA value of illite and kaolinite are 75 and 100, respectively (Nesbitt and Young, 1982, 1984, 1989). The CIA values for loess samples from Majs 2/a section ranged between 61 and 65, from Majs 2/b

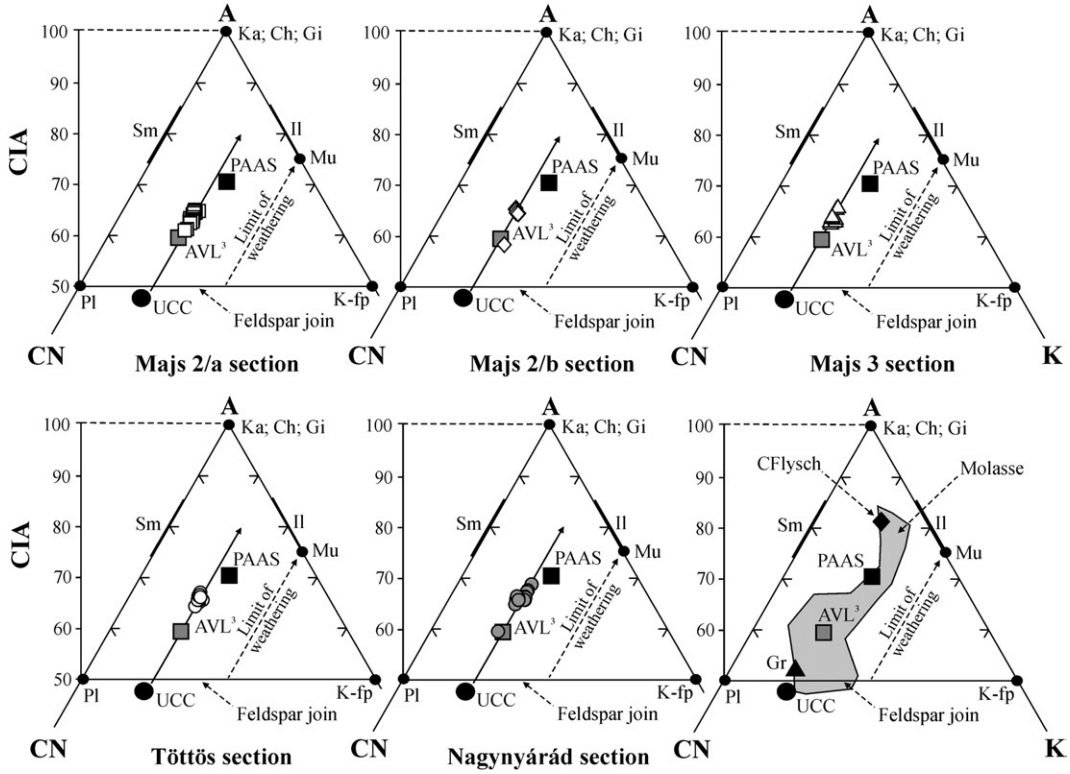

Figure 7. Ternary A–CN–K diagrams of the studied loess deposits (in molar proportions). The samples plotted subparallel to the A–CN join, suggesting an ideal weathering of a slightly more felsic source than the UCC. Symbols are as follows Sm: Smectite, Il: Illite, Mu: muscovite, Ka: Kaolinite, Ch: Chlorite, Gi: Gibbsite, Pl: Plagioclase, K-fp: K-feldspar, and others as in Fig. 4. Note only the top 50% of the triangle is shown.

https://doi.org/10.1016/j.yqres.2008.02.001 Published online by Cambridge University Press

between 58 and 65, and from Majs 3 between 62 and 66 with an average of 64 for all (Table 1). The loess samples from Töttös and Nagynyárád sections had slightly higher CIA values than the Majs sections and ranged between 64 and 67 and between 60 and 69, respectively, with an average of 66 for both (Table 1).

There was no clear distinction among the different sections studied, which might suggest a similar alteration history for these loess deposits. The CIA values were in the range of 58–69, which was higher than the UCC value of 48 (Taylor and McLennan, 1985) and the AVL[3] value of 59, but it was slightly lower than the PAAS value of 70 (Taylor and McLennan, 1985). The relatively low and restricted CIA values suggested a weak to moderate degree of chemical weathering in the source area where clay minerals were dominated by illite and/or smectite (Gallet et al., 1998).

Fresh rock composition and paleo-weathering conditions

Weathering trends for our loess sections plotted in the relatively less-weathered region on molar proportions diagram (Nesbitt and Young, 1984, 1989) of Al_2O_3–CaO^*+Na_2O–K_2O (A–CN–K) for all samples (Fig. 7). A simple weathering trend was defined (solid line with arrow), which was subparallel to the A–CN boundary, primarily because removal rates of Na and Ca from plagioclase generally were greater than the removal rate of K from K-feldspar (Nesbitt and Young, 1984, 1989; Nesbitt et al., 1997). The starting point of the weathering trend was close to the composition of the UCC (Taylor and McLennan, 1985), which represents a composition nearly equivalent to the igneous rock type granodiorite (Taylor and McLennan, 1985; McLennan, 2001), with a small displacement towards the position of K-feldspar (Fig. 7). This supported that the present samples were derived from a felsic source area, following a trend from a slightly more K-feldspar-rich fresh rock composition than that of the UCC. The degree of weathering was variable within the individual suites (except for Majs 3 and Töttös sections), producing weak scatter along the trend. This pattern is typical of non-steady state weathering conditions, where active tectonism permits erosion of all zones within weathering profiles developed on source rocks (Nesbitt et al., 1997).

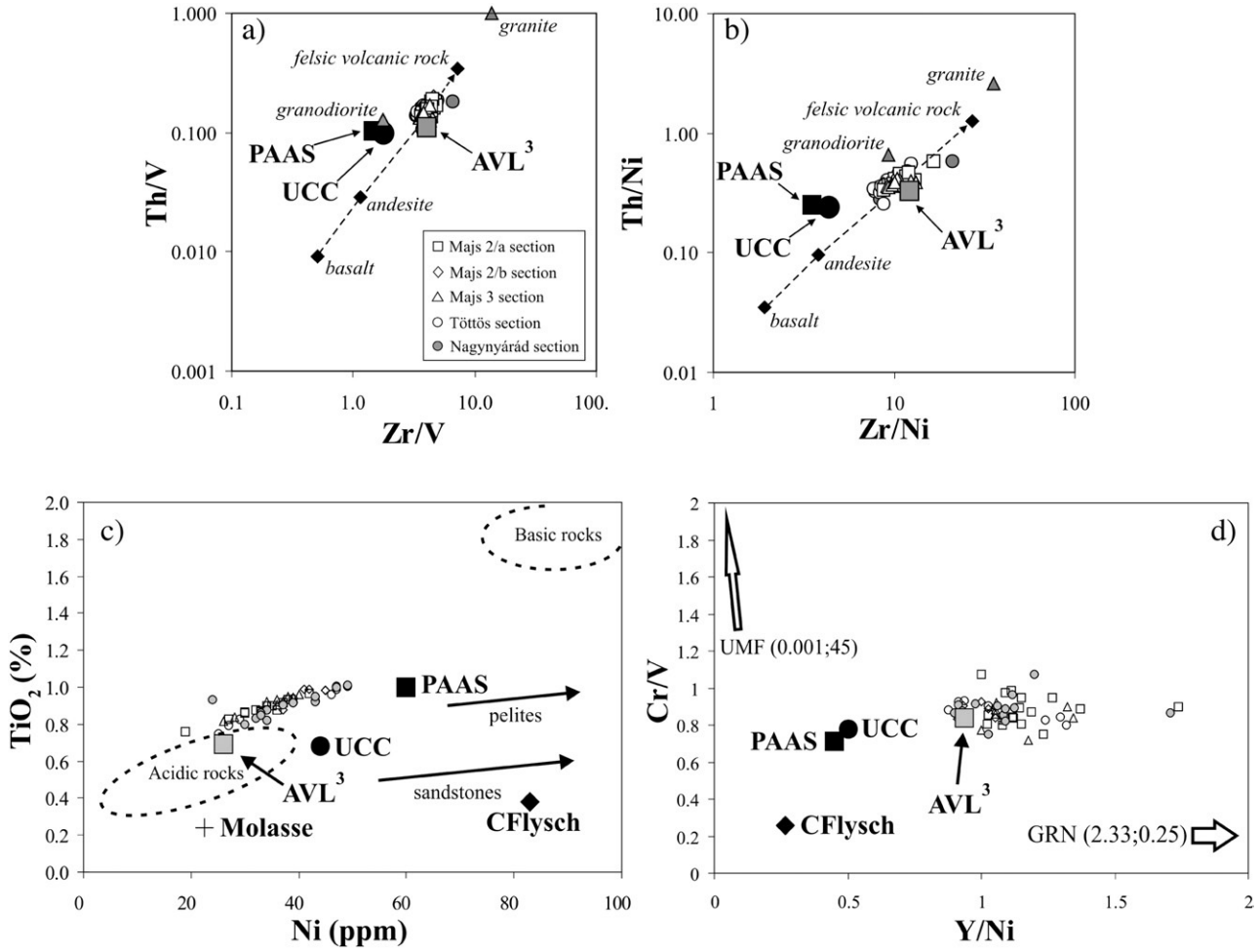

Figure 8. Plots of a) Th/V vs. Zr/V, b) Th/Ni vs. Zr/Ni, and provenance discrimination diagrams of c) TiO_2 vs. Ni (Floyd et al., 1989) and d) Cr/V vs. Y/Ni (Hiscott, 1984), comparing the studied loess samples from southwestern Hungary and average loess composition (AVL[3]; Table 2), post-Archean Australian average shale (PAAS; Taylor and McLennan, 1985; McLennan, 2001), Upper Continental Crust (UCC; Taylor and McLennan, 1985). Igneous rock compositions on a) and b) are average values from Condie (1993). On c) and d) the samples were also contrasted to Carpathian flysch sediments (CFlysch; Adamova, 1991) and sandstones from the Central Alps (Molasse; von Eynatten, 2003) as potential source material, and to ultramafic rock (UMF) and granite (GRN) compositions (Amorosi et al., 2002).

https://doi.org/10.1016/j.yqres.2008.02.001 Published online by Cambridge University Press

The samples from Majs 3 and Töttös sections were tightly clustered but stayed on the same trend as the other sections (Fig. 7). These characteristics suggested that these two sections were derived from source materials that had similar lithologies to the other studied sections but were more weathered. The weathering here was close to steady state conditions, in which the material removal rate matched the production of mineralogically and chemically uniform weathering products (Nesbitt et al., 1997). An alternative interpretation was that the CIA indices for Majs 3 and Töttös sections reflect sediment recycling (Hassan et al., 1999). It is possible, however, that different parts of the Young Loess Series have been exposed in the loess sections studied, representing somewhat different time intervals.

A more humid climate might have been present at Töttös and Nagynyárád locations during loess-forming processes, because the CIA values were slightly higher than in Majs loess samples. More intense weathering was further comfirmed by humic loess (or embryonic soil) lithology from the Nagynyárád section (Újvári, 2005). However, no systematic change of CIA values was observed among the compared samples (Table 1). In addition, Sr-depletion, Rb/Sr and Ba/Sr ratios of Nagynyárád section did not give distinct information on the pedogenetic intensity (Fig. 6 and Table 1).

The majority of the data points plotted between the AVL^3 and PAAS in a very well-defined region (Fig. 7). However, other potential parent materials such as flysch and granite from Western Carpathians plotted away from the samples and there were differences observed between the samples and molasse sandstones, representing a Central Alpine provenance area (Fig. 7).

The granite from the Western Carpathians (Broska et al., 2002) has relatively low CIA value, corresponding to the typical igneous compositions. The Carpathian flysch (Adamova, 1991) plotted along the inferred weathering trend for the loess samples, however, in a position consistent with derivation from highly weathered felsic rocks. So it is unlikely that the Hungarian loess deposits represent weathering products of these flysch sediments. The molasse sandstone data (von Eynatten, 2003) exhibited a broad range of the CIA values and suggested a weathering trend towards an illite composition (Fig. 7), possibly as a result of a metasomatic increase in K during diagenesis (Fedo et al., 1995). This pattern may indicate mixing of a highly to moderately weathered source with an unweathered source of different primary composition.

All these observations of non-steady state A–CN–K relations were consistent with the reconstruction of the active tectonism in the Pleistocene by Horváth and Cloetingh (1996) and Székely et al. (2002). Deepening of the Pannonian Basin was apparently also accompanied by temporary establishments of steady state weathering conditions, suggestive of a hiatus in Alpine–Carpathian source uplift. On the other hand, A–CN–K relations (Fig. 7), together with the geochemical homogeneity in the loess sections (Figs. 4 and 5), reflect a uniform source region and suggested that the dust material of these Pleistocene sediments might have been at least partially recycled and well homogenized during transport.

Mineral sorting and characterization of source components

The loess deposits in southwestern Hungary had significantly higher abundances of TiO_2, P_2O_5, Th, Zr, Nb, La, Ce, and Y than the UCC (Fig. 4 and 5). This observation suggested that, in a general sense, the distribution of these elements was transport-controlled within our data set (Table 1) because the elements concentrated in heavy mineral suites (e.g., zircon, rutile, tourmaline, apatite, garnet, chromite, magnetite, ilmenite, etc.) may be strongly fractionated during mineral sorting of clastic sediments (Taylor et al., 1983; Taylor and McLennan, 1985; McLennan, 1989, 2001; Preston et al., 1998).

The possibility of heavy mineral enrichment was tested using Th/V vs. Zr/V, and Th/Ni vs. Zr/Ni ratios (Fig. 8a–b), which in addition to Cr/V and Y/Ni ratios are good overall indicators of igneous chemical differentiation processes (Hiscott, 1984; Taylor and McLennan, 1985; Tripathi and Rajamani, 1999; McLennan, 2001; Amorosi et al., 2002). Additionally, compatible trace elements such as Cr are useful in identifying accessory detrital components such as chromite, commonly derived from mafic to ultramafic sources including ophiolites, not readily recognized by petrography alone (Zimmermann and Bahlburg, 2003; Mikes et al., 2006). The Th/V vs. Zr/V and Th/Ni vs. Zr/Ni data intersected a primary compositional trend (Fig. 8a and b; dashed line with arrow) defined by igneous rocks at high Zr/metal ratio (Condie, 1993), above the average value of UCC and PAAS. The elements Th and Zr are enriched in felsic rather than in mafic rocks, because they are highly incompatible during most igneous melting and fractionation processes (Taylor and McLennan, 1985; McLennan, 2001). High Zr/V and Zr/Ni ratios suggested zircon enrichment in these sediments, which is an indication of well-mixed and recycled dust source. This also supported by the fact that our data plotted close to the AVL^3 composition in a very defined region (Fig. 8a–b).

The above interpretation was additionally supported by TiO_2 vs. Ni (Floyd et al., 1989) and Cr/V vs. Y/Ni provenance diagrams (Hiscott, 1984; McLennan et al., 1993) (Fig. 8c–d). The loess sample values corresponded to the composition of acidic rocks as plotted close to AVL^3. Lower Ni content and higher Y/Ni ratios were detected in the loesses than in the UCC and PAAS. Nickel is positively correlated with TiO_2 (Fig. 8c), suggesting that it might be bound in Ti-bearing phyllosilicates. Nevertheless, the general depletion of compatible elements such as Cr, V, and Ni (Figs. 5 and 8c) supported the fact that the amounts of mafic or ultramafic rocks were insignificant in the source area (Taylor and McLennan, 1985; Floyd et al., 1989; Tripathi and Rajamani, 1999). As for the ultrabasic source components, therefore, derivation from the Penninic ophiolite of the eastern Alps is improbable.

Apatite, rutile and monazite could also have been selectively picked up by winds from a felsic provenance area along with zircon due to their smaller grain sizes. This result is consistent with the suggestion that eolian sedimentary transport processes involved with loess formation lead to significant heavy mineral (especially “ultrastable” heavy mineral) enrichments (Taylor et al., 1983; Schnetger, 1992; Gallet et al., 1996). Based on

https://doi.org/10.1016/j.yqres.2008.02.001 Published online by Cambridge University Press

geochemical homogeneity and stable heavy mineral population dominated by zircon, the present samples are consistent with a felsic magmatic and/or reworked sedimentary source (Figs. 4 and 5).

Dust provenance interpretation

The origin of loess particles and the mode of formation for Hungarian loess deposits have long been a controversial issue (Smalley and Leach, 1978; Smith et al., 1991; Wright, 2001). The primary fluvial transport was carried out by the Danube and Tisza rivers, which transported weathered materials from the Alps and Carpathians into the Pannonian Basin from the NW and the NE, respectively. The secondary eolian transport was determined by the prevailing wind directions, which were northerly–northeasterly winds in the summer and westerly winds in the winter during the Weichselian glacial maximum in Europe (Meyer and Kottmeier, 1989). The wind directions were possibly similar during the Pleistocene glaciations in the Pannonian Basin because high pressure centres located over the Scandinavian ice sheet and the main glaciers likely produced northerly anticyclonic winds (Hobbs 1943). Recent studies of anisotrophy of magnetic susceptibility (AMS) in loess of middle Pleistocene age support this idea (Bradák 2006, in press). Bradák (in press) has revealed NE–SW paleo-wind direction from the loess overlying the Bag Tephra (>380 ka; Pouclet et al., 1999) in case of 3 sections at Gödöllő Hills, eastwards from the capital town of Budapest (Fig. 1a), N–S direction at Basaharc (North-Hungary) and NW–SE direction at Sióagárd (Middle-Hungary, Transdanubia). The unveiled paleo-wind directions at Transdanubia seem to be in good agreement with the results of Jámbor (2002) who determined the main Pleistocene wind tunnels on the basis of ventifact occurrences in Hungary. However, the revealed directions at Gödöllő Hills deviate from each other (NE–SW versus NW–SE; Fig. 1a).

Significant differences were detected between the UCC-normalized major and trace element distributions of the samples and the potential source components (Figs. 4f and 5f), which pattern might have derived from a multicomponent mixing of dust particles during sedimentary processes. The role of fluvial transport was clearly proven by the Na_2O/Al_2O_3 vs. K_2O/Al_2O_3 diagram (Fig. 3d), reflecting that the loess protoliths must have experienced at least one cycle of aquatic sedimentary differentiation processes. Also, the results of the A–CN–K relationship (Fig. 7) and Th/metal vs. Zr/metal diagrams (Fig. 8a–b) suggest that the source material of these Pleistocene sediments must have been at least partially recycled and well homogenized during fluvial and subsequent eolian transports.

Unfortunately, the geochemical analyses and description of the relatively well-known Pannonian sedimentary units in the Pannonian Basin (Rónai, 1985) have not been completed, which complicates the determination of the dust provenance areas of this region. At this point, we can only hypothesize that the loess deposited by both fluvial and eolian processes, either from materials with uniform composition or from various sources, underwent geological mixing processes prior to loess deposition, as did the Pannonian sediments. On the basis of whole-rock chemical data we can neither confirm nor confute the connection between the former supposed provenance areas or potential source rocks and the studied loesses.

Global average loess composition

Loess deposits can provide us with a natural sampling of large regions of surficial crust (Taylor et al., 1983), because they are widespread and made by several mechanisms which produce silt-sized particles (e.g., glacial grinding, desert weathering and deflation, "mountain loess" process operating with high energy transfer and frequent freeze–thaw conditions) in various sedimentary environments (Gallet et al., 1998; Tripathi and Rajamani, 1999; Wright, 2001). These characteristics make loess suitable for estimating the average chemical composition of the UCC (Taylor et al., 1983); however, the composition of loess cannot be used directly to infer UCC composition. It is a difficult process and only some elemental ratios can be used for that purpose (McLennan, 2001).

Our loess data were quite homogenous in both major and trace element chemistry (Table 1, Figs. 4 and 5), but differed from the average loess composition—AVL^3—in TiO_2, MgO, CaO, Th, Nb, La, Ce, and Y (Figs. 4f and 5f). Strong regional variations were detected by comparing the average composition of our samples (HUN^3; Table 2) and some individual geochemical parameters (Figs. 3a–c and 6) of our results to AVL^3. These findings indicated that the previously estimated average loess compositions (e.g., Schnetger, 1992; McLennan, 2001; AVL^3, Table 2) could be complemented with our results to provide a more accurate average loess estimation. Therefore, we reevaluated the published worldwide loess regional averages (Table 2) to calculate a new global average loess composition (GAL), which resulted in somewhat lower SiO_2 content and somewhat higher TiO_2, Al_2O_3, FeO_{tot}, MgO, CaO, Pb, Th, Zr, Nb, La, Ce, and Y abundances than in AVL^3.

Conclusions

All the loess samples from southwestern Hungary have nearly uniform chemical composition, suggesting a roughly similar alteration history of these deposits. The relatively low and restricted CIA values (58–69) suggest a weak to moderate degree of chemical weathering in a felsic source area. The A–CN–K pattern of the Majs 2/a, Majs 2/b, and Nagynyárád profiles is typical of non-steady state weathering conditions, indicating active tectonism of the Alpine–Carpathian System during the Pleistocene.

The whole-rock TiO_2, P_2O_5, Th, Zr, Nb, Y, La, and Ce budgets of the samples are controlled by the abundances and compositions of the heavy minerals such as zircon, rutile, apatite, and monazite derived from felsic magmatic and/or reworked sedimentary sources. Source material of these Pleistocene loess deposits must have been at least partially recycled and well homogenized during fluvial and subsequent eolian transport processes. Therefore, an accurate determination of provenance areas based on whole-rock geochemistry cannot be made.

https://doi.org/10.1016/j.yqres.2008.02.001 Published online by Cambridge University Press

Acknowledgments

The authors are grateful for the field assistance from Antal Újvári and Ferenc Varga. We wish to thank Szabolcs Czigány for his help with sample preparation and the GeoAnalytical Laboratory of Washington State University for the sample analysis by XRF. We also greatly thank Martha Godchaux, and two anonymous reviewers for improving our manuscript with their constructive criticism.

References

Adamova, M., 1991. Geochemistry of flysch sediments and its application in geological interpretations. Geologica Carpathica 42, 147–156.

Amorosi, A., Centineo, M.C., Dinelli, E., Lucchini, F., Tateo, F., 2002. Geochemical and mineralogical variations as indicators of provenance changes in late quaternary deposits of SE Po Plain. Sedimentary Geology 151, 273–292.

Bock, B., McLennan, S.M., Hanson, G.N., 1998. Geochemistry and provenance of the Middle Ordovician Austin Glen Member (Normanskill Formation) and the Taconian Orogeny in New England. Sedimentology 45, 635–655.

Bradák, B., 2006. Meghatározható-e a paleoszélirány löszfeltárásokból a mágneses szuszceptibilitás anizotrópia (AMS) vizsgálatával? Válaszok Bulla Bélának. Földrajzi közlemények 130, 185–198 (in Hungarian with English abstract).

Bradák, B., in press. Application of anisotropy of magnetic susceptibility (AMS) for the determination of paleo-wind directions and paleo-environment during the accumulation period of Bag Tephra, Hungary. Quaternary International. DOI:10.1016/j.quaint.2007.11.005.

Broska, I., Williams, C.T., Uher, P., Konečný, P., Leichmann, J., 2002. The geochemistry of phosphorus in different granite suites of the Western Carpathians, Slovakia: the role of apatite and P-bearing feldspar. Chemical Geology 205, 1–15.

Condie, K.C., 1993. Chemical composition and evolution of the upper continental crust: Contrasting results from surface samples and shales. Chemical Geology 104, 1–37.

Csontos, L., Nagymarosy, A., Horváth, F., Kovács, M., 1992. Tertiary evolution of the Intra-Carpathian area: a model. Tectonophysics 208, 221–241.

Csontos, L., Benkovics, L., Bergerat, F., Mansy, J., Wórum, G., 2002. Tertiary deformation history from seismic section study and fault analysis in a former European Tethyan margin (the Mecsek–Villány area, SW Hungary). Tectonophysics 357, 81–102.

Ding, Z.L., Sun, J.M., Yang, S.L., Liu, T.S., 2001. Geochemistry of the Pliocene red clay formation in the Chinese Loess Plateau and implications for its origin, source provenance and paleoclimate change. Geochimica et Cosmochimica Acta 65, 901–913.

von Eynatten, H., 2003. Petrography and chemistry of sandstones from the Swiss Molasse Basin: an archive of the Oligocene and Miocene evolution of the Central Alps. Sedimentology 50, 703–724.

Fedo, C.M., Nesbitt, H.W., Young, G.M., 1995. Unraveling the effects of potassium metasomatism in sedimentary rocks and paleosols, with implications for paleoweathering conditions and provenance. Geology 23, 921–924.

Floyd, P.A., Winchester, J.A., Park, R.G., 1989. Geochemistry and tectonic setting of Lewisian clastic metasediments from the early Proterozoic Loch Maree Group of Gairloch, N. W. Scotland. Precambrian Research 45, 203–214.

Gallet, S., Jahn, B., Torii, M., 1996. Geochemical characterization of the Luochuan loess-paleosol sequence, China, and paleoclimatic implications. Chemical Geology 133, 67–88.

Gallet, S., Jahn, B., Van Vliet Lanoë, B., Dia, A., Rossello, E., 1998. Loess geochemistry and its implications for particle origin and composition of the upper continental crust. Earth and Planetary Science Letters 156, 157–172.

Garrels, R.M., Mackenzie, F.T., 1971. Evolution of Sedimentary Rocks. Norton & Company, New York, p. 397.

Hassan, S., Ishiga, H., Roser, B.P., Dozen, K., Naka, T., 1999. Geochemistry of Permian–Triassic shales in the Salt Range, Pakistan: implications for provenance and tectonism at the Gondwana margin. Chemical Geology 158, 293–314.

Hädrich, F., 1975. Zur Methodik der Lössdifferenzierung auf der Grundlage der Carbonatverteilung. Eiszeitalter und Gegenwart 26, 95–117.

Hiscott, R.N., 1984. Ophiolitic source rocks for Taconic-age flysch: trace-element evidence. GSA Bulletin 95, 1261–1267.

Hobbs, H.W., 1943. The glacial anticyclones and the European continental glacier. American Journal of Science 241, 333–336.

Horváth, F., Cloetingh, S., 1996. Stress-induced late-stage subsidence anomalies in the Pannonian Basin. Tectonophysics 266, 287–300.

Hum, L., 1998a. Geochemical investigations of the Dunaszekcső loess-paleosoil sequence. Acta Mineralogica-Petrographica (Szeged) 39, 139–150.

Hum, L., 1998b. Délkelet-Dunántúli lösz-paleotalaj sorozatok keletkezésének rekonstrukciója üledéktani, geokémiai és őslénytani vizsgálatok alapján. Ph. D. Thesis, József Attila University, Szeged, 140 p (in Hungarian with English summary).

Hum, L., 2002. Délkelet-dunántúli löszösszletek ásványos és geokémiai jellegei és ezek eredete. Földtani Közlöny 132, 117–132 (különszám, in Hungarian with English abstract).

Hum, L., Fényes, J., 1995. The geochemical characteristics of loesses and paleosols in the South-Eastern Transdanube (Hungary). Acta Mineralogica-Petrographica (Szeged) 36, 89–100.

Jahn, B., Gallet, S., Han, J., 2001. Geochemistry of the Xining, Xifeng and Jixian sections, Loess Plateau of China: eolian dust provenance and paleosol evolution during the last 140 ka. Chemical Geology 178, 71–94.

Jámbor, Á., 2002. A magyarországi pleisztocén éleskavics előfordulások és földtani jelentőségük. Földtani Közlöny 132, 101–116 (különszám, in Hungarian with English summary).

Johnson, D.M., Hooper, P.R., Conrey, R.M., 1999. XRF analysis of rocks and minerals for major and trace elements on a single low dilution Li-tetraborate fused bead. Advances in X-ray Analysis 41, 843–867.

Lautridou, J.P., Sommé, J., Jamagne, M., 1984. Sedimentological, mineralogical and geochemical characteristics of the loesses of North-West France. In: Pécsi, M. (Ed.), Lithology and Stratigraphy of Loess and Paleosols. Geographical Research Institute of the Hungarian Academy of Sciences, Budapest, pp. 121–132.

McLennan, S.M., 1989. Rare earth elements in sedimentary rocks: influence of provenance and sedimentary processes. In: Lipin, B.R., McKay, G.A. (Eds.), Geochemistry and Mineralogy of Rare Earth Elements. MSA, Reviews in Mineralogy, 21, pp. 169–200.

McLennan, S.M., 1993. Weathering and global denudation. Journal of Geology 101, 295–303.

McLennan, S.M., 2001. Relationships between the trace element composition of sedimentary rocks and upper continental crust. Geochemistry, Geophysics, Geosystems 2, 24, 2000GC000109.

McLennan, S.M., Hemming, S., McDaniel, D.K., Hanson, G.N., 1993. Geochemical Approaches to Sedimentation, Provenance and Tectonics. In: Johnsson, M.J., Basu, A. (Eds.), Processes Controlling the Composition of Clastic Sediments, Geological Society of America Special Paper, 284, pp. 21–40.

Meyer, H.-H., Kottmeier, Ch., 1989. The atmospheric circulation in Europe during the Weichselian Pleniglacial — as derived from palaeowind indicators and model simulations. Eiszeitalter und Gegenwart 39, 10–18 (in German with English summary).

Mikes, T., Dunkl, I., Frisch, W., von Eynatten, H., 2006. Geochemistry of Eocene flysch sandstones in the NW External Dinarides. Acta Geologica Hungarica 49, 103–124.

Nesbitt, H.W., Young, G.M., 1982. Early Proterozoic climates and plate motions inferred from major element chemistry of lutites. Nature 299, 715–717.

Nesbitt, H.W., Young, G.M., 1984. Prediction of some weathering trends of plutonic and volcanic rocks based on thermodynamic and kinetic considerations. Geochimica et Cosmochimica Acta 48, 1523–1534.

Nesbitt, H.W., Young, G.M., 1989. Formation and diagenesis of weathering profiles. Journal of Geology 97, 129–147.

Nesbitt, H.W., Fedo, C.M., Young, G.M., 1997. Quartz and feldspar stability, steady and nonsteady-state weathering, and petrogenesis of siliciclastic sands and muds. Journal of Geology 105, 173–191.

Pécsi, M., 1967. A löszfeltárások üledékeinek genetikai osztályozása a Kárpát-medencében. Földrajzi Értesítő 16, 1–18 (in Hungarian).

Pécsi, M., 1990. Loess is not just the accumulation of dust. Quaternary International 7/8, 1–21.

Pécsi, M., 1993. Loess and the Quaternary. Akadémiai Kiadó, Budapest, p. 375.
Pécsi, M., 1995. Loess stratigraphy and Quaternary climatic change. In: Pécsi, M., Schweitzer, F. (Eds.), Concept of loess, loess-paleosol stratigraphy. Loess in Form 3, pp. 23–30.
Pécsi-Donáth, É., 1985. On the mineralogical and pedological properties of the younger loess in Hungary. In: Pécsi, M. (Ed.), Loess and the Quaternary. Akadémiai Kiadó, Budapest, pp. 93–104.
Pouclet, A., Horváth, E., Gábris, Gy., Juvigné, E., 1999. The Bag Tephra, a widespread tephrochronological marker in Middle Europe: chemical and mineralogical investigations. Bulletin of Volcanology 60, 265–272.
Preston, J., Hartley, A., Hole, M., Buck, S., Bond, J., Mange, M., Still, J., 1998. Integrated whole-rock trace element geochemistry and heavy mineral chemistry studies: aids to the correlation of continental red-bed reservoirs in the Beryl Field, UK North Sea. Petroleum Geoscience 4, 7–16.
Pye, K., 1983. Grain surface textures and carbonate content of late Pleistocene loess from West Germany and Poland. Journal of Sedimentary Petrology 53, 973–980.
Roddaz, M., Viers, J., Brusset, S., Baby, P., Boucayrand, C., Hérail, G., 2006. Controls on weathering and provenance in the Amazonian foreland basin: insights from major and trace element geochemistry of Neogene Amazonian sediments. Chemical Geology 226, 31–65.
Rónai, A., 1985. The Quaternary of the Great Hungarian Plain. In: Pécsi, M. (Ed.), Loess and the Quaternary. Akadémiai Kiadó, Budapest, pp. 51–63.
Schellenberger, A., Veit, H., 2006. Pedostratigraphy and pedological and geochemical characterization of Las Carreras loess–paleosol sequence, Valle de Tafi, NW-Argentina. Quaternary Science Reviews 25, 811–831.
Schnetger, B., 1992. Chemical composition of loess from a local and worldwide view. Neues Jahrbuch für Mineralogie Monatshefte 1, 29–47.
Shackleton, N.J., Berger, A., Peltier, W.R., 1990. An alternative astronomical calibration of the lower Pleistocene timescale based on ODP Site 677. Transactions of the Royal Society of Edinburgh - Earth Sciences 81, 251–261.
Smalley, I.J., Leach, J.A., 1978. The origin and distribution of loess in the Danube Basin and associated regions of East-Central Europe — a review. Sedimentary Geology 21, 1–26.
Smith, B.J., Wright, J.S., Whalley, W.B., 1991. Simulated aeolian abrasion of Pannonian sands and its applications for the origins of the Hungarian loess. Earth Surface Processes and Landforms 16, 745–752.
Sun, J., 2002. Provenance of loess material and formation of loess deposits on the Chinese Loess Plateau. Earth and Planetary Science Letters 203, 845–859.
Sümeghy, J., 1953. Medencéink pliocén és pleisztocén rétegtani kérdései. A MÁFI évi jelentése az 83–109 (1951. évről, in Hungarian).
Székely, B., Reinecker, J., Dunkl, I., Frisch, W., Kuhlemann, J., 2002. Neotectonic movements and their geomorphic response as reflected in surface parameters and stress patterns in the Eastern Alps. In: Cloetingh, S.A. P.L., Horváth, F., Bada, G., Lankreijer, A.C. (Eds.), Neotectonics and Surface Processes: The Pannonian Basin and Alpine/Carpathian System. EGU Stephan Mueller Special Publication Series 3, pp. 149–166.
Taylor, S.R., McLennan, S.M., 1985. The Continental Crust: its Composition and Evolution. Blackwell Scientific Publications Ltd., p. 312.
Taylor, S.R., McLennan, S.M., McCulloch, M.T., 1983. Geochemistry of loess, continental crustal composition and crustal model ages. Geochimica et Cosmochimica Acta 47, 1897–1905.
Tripathi, J.K., Rajamani, V., 1999. Geochemistry of the loessic sediments on Delhi ridge, eastern Thar desert, Rajasthan: implications for exogenic processes. Chemical Geology 155, 265–278.
Újvári, G., 2005. Dél-baranyai lösz-paleotalaj sorozatok szedimentológiai, geokémiai és malakológiai vizsgálata. Ph.D. Thesis, University of Pécs, 220 p. (in Hungarian with English abstract).
Wright, J.S., 2001. “Desert” loess versus “glacial” loess: quartz silt formation, source areas and sediment pathways in the formation of loess deposits. Geomorphology 36, 231–256.
Wright, J.S., Smith, B., Whalley, B., 1998. Mechanisms of loess-sized quartz silt production and their relative effectiveness: laboratory simulations. Geomorphology 23, 15–34.
Zimmermann, U., Bahlburg, H., 2003. Provenance analysis and tectonic setting of the Ordovician clastic deposits in the southern Puna Basin, NW Argentina. Sedimentology 50, 1079–1104.